1 of 1

Conf-940598--2

PNL-SA-22934

EFFECT OF PRE-WELDING HEAT-TREATMENTS ON WELDING A TWO-PHASE Ni_3Al ALLOY

H. Li[a]
R. H. Jones

May 1994

Presented at the
International Conference on High-Temperature Intermetallics
May 16-19, 1994
San Diego, California

Prepared for
the U.S. Department of Energy
under Contract DE-AC06-76RLO 1830

Pacific Northwest Laboratory
Richland, Washington 99352

(a) Associated Western Universities - NW, Richland, Washington

Effect of Pre-Welding Heat-Treatments on Welding a Two-Phase Ni_3Al Alloy

Huaxin Li* and R. H. Jones**

* Associated Western Universities—NW, c/o P.O. Box 999, P8-15, Richland, WA 99352

Phone: 509-376-4529 Fax: 509-376-0418

** Pacific Northwest Laboratory, P.O. Box 999, M.S. P8-15, Richland, WA 99352

Abstract

Autogenous gas-tungsten arc welding was performed on a two-phase Ni_3Al alloy. Plates 3 mm thick were cut from a cast ingot and were subjected to three pre-welding heat treatments (PWHT), namely, as-cast, annealed at 1100°C for 23 h (HT1) and HT1 plus 1120°C/30 min/air cool (HT2). The as-cast alloy was characterized by dendrites with many eutectic cells located at dendrite boundaries (DBs). The eutectic cells were destroyed by HT1. However, HT2 make no further changes on microstructure. Analysis by energy dispersive X-ray spectroscopy (EDX) revealed that the DBs of as-cast alloy were enriched with Zr. The Zr enrichment at DBs was increased further by HT1 and HT2. No solidification crack visible to the unaided eye was found in either the fusion zone (FZ) or the heat-affected zone (HAZ) due to welding. The FZ consisted of columnar grains with a eutectic structure along the boundaries. The eutectic structure was enriched with Zr and contained many microcracks and some Zr-rich phases. Micro-solidification cracks were occasionally found along boundaries in FZ. The alloy was sensitive to liquation cracks that occurred along DBs in the HAZ. While PWHT had no effect on the characteristics of the FZ, PWHT had a notable effect on the severity of liquation cracking. The average crack numbers per 5 cm weldment were 12 for as-cast, 14 for HT1, and 17 for HT2. The role of Zr-inducing solidification cracks in FZ and liquation cracks in HAZ is discussed.

1. Introduction

Nickel aluminide, Ni_3Al, is an ordered intermetallic compound with a $L1_2$-type crystal structure. It has attractive mechanical properties and good oxidation resistance at high temperatures. The yield strength [1] of single-crystal Ni_3Al initially increases with the temperature, reaches a maximum at about 650°C, and then starts to decrease. But polycrystalline Ni_3Al is severely brittle and undergoes intergranular fracture [2]. Adding a minute amount of B (a few hundred wt ppm) improves ductility in Ni-rich Ni_3Al tremendously [3,4]. Besides B, small amounts (less than 1 wt%) of Zr or Hf are added [5] in Ni_3Al alloys to provide solid solution strengthening and creep resistance. Recently, a series of advanced Ni_3Al alloys alloyed with B, Zr, Cr, and Mo have been developed [5-7] at Oak Ridge National Laboratory (ORNL), TN. High-temperature strength and creep resistance of these advanced nickel aluminides have been demonstrated to be superior to most of the common commercial heat-resistance alloys [7].

In developing a commercial alloy, weldability is a key issue because joining by a conventional welding process is an important means of fabricating engineering alloys into structural components. David and coworkers [8,9] have performed autogenous gas-tungsten-arc (GTA) and electron-beam (EB) welding on several ductile Ni_3Al alloys, some containing Fe. The specimens were made by arc melting followed by repeated rolling and annealing. They concluded that ductile Ni_3Al is highly susceptible to hot cracking in the heat-affected zone (HAZ) and that the cracks are along grain boundaries. They made successful joints only with EB welding operated within a narrow range of welding speeds and beam focus conditions. Later, Santella et al. [10] reported crack-free GTA and EB welds in a Ni_3Al alloy containing 0.1-at% B and 0.5-at% Hf. The welding was successful in the repeatedly rolled and extruded alloy, but not in the cast alloy. To reduce the cost of Ni_3Al alloys, Hf was replaced with Zr. Li et al. [11] first reported that IC-50, a single-phase Ni_3Al containing 0.5-wt% Zr, was highly sensitive to liquation cracking in the HAZ and solidification cracking in the fusion zone (FZ). They found later that

liquation cracking was prevailing in the HAZ, not only in the single phase Ni_3Al alloy [12,13], but also in a two-phase Ni_3Al alloy containing Cr and Mo, such as IC-396M [13,14]. Liquation cracking was caused by grain-boundary incipient melting, which was due to Zr enrichment at grain boundaries in these alloys. Adding Cr improved the resistance to solidification cracking in FZ, but exerted little effect on liquation cracking in the HAZ [13,14]. It was also found by Li [15] that the grain-boundary melting temperature of Ni_3Al alloys containing Zr depended slightly on the thermal history. This study was an attempt to exploit the effect of pre-welding heat treatments on liquation cracking in the HAZ of IC-218, a two-phase Ni_3Al alloy containing Cr and Zr.

2. Materials and experimental methods

A two-phase Ni_3Al alloy, designated as IC-218, used in this study was designed and developed by ORNL, TN. The ingots were made by investment casting and were provided by Armco Inc., OH. The chemical compositions (as provided by the supplier) were 8.65 Al-7.87 Cr-0.86 Zr-0.02 B and Ni (by wt%) or 16.98 Al-8.02 Cr-0.51 Zr-0.10 B and Ni (by at%). Welding coupons of approximately 60 mm x 15 mm x 3 mm were cut from the ingots with a silicon carbide cutting wheel and were ground to remove oxide films and sharp edges. Three pre-welding heat treatments were used in this study: as-cast, 1100°C/23 h/ furnace cool (HT1), and HT1 plus 1120°C/30 min/air cool (HT2). Fully-penetrated weldments were made by a gas tungsten arc welder in alternating current mode. The welding parameters were as follows: current - 50 A, voltage - 12 V, argon flow rate - 25 m^3/h, and welding speed - 12 cm/min. Tungsten rods (2.4 mm diameter thoriated [2 wt%]) were used to increase the electron-emission rate. The welding was autogenous, i.e., no filler metal was used. Three weldments with a length of about 50 mm were made for each heat-treatment condition.

All weldments were ground with emery paper, polished with alumina slurry, and etched with an etchant that contained 40 mL HCl, 30 mL HNO_3, 20 mL glacial acetic acid, and 10 mL glycerol. The microstructure of the specimens was examined by an optical microscopy and a scanning electron microscopy (SEM). The local chemical composition was analyzed by energy-dispersive x-ray (EDX) spectroscopy.

3. Results and discussion

3.1. Characterization of Base Materials

The microstructure of as-cast IC-218 was characterized by the dendrites with many eutectic cells, as shown in Fig. 1a. According to the Ni-Al-Cr solidification diagram [16], during casting, the main and secondary dendritic arms with a disordered fcc structure (γ phase) developed first, then the remaining liquid underwent a eutectic reaction (Liquid $\rightleftarrows \gamma' + \gamma$), where γ' is a $L1_2$-type ordered phase; as cooling continued, most of the γ phase transformed to γ'. The volume fraction of γ phase in IC-218 equilibrated at room temperature was about 10–15%, as reported by Liu et al. [5]. The average spacing of main dendrites was 834 ± 345 μm. Some cast porosity and precipitates appeared. The porosity was mainly located at the edges of the eutectic cells. Most of the precipitates were cuboidal, and a few were triangular (Fig. 1a). The precipitates could be found everywhere, and their mean edge length was 3.9 ± 1.1 μm. An analysis by microprobe [15] showed that the particles contained 30 at% Zr and 65 at% O, indicating that the particles were ZrO_2. Analyses of the eutectic cells by EDX showed a clear Zr peak at the edges of the eutectic cells and a weak Zr peak in the cores of the cells, suggesting that Zr was enriched at the edges of the eutectic cells. It will be seen later that some liquation cracks occurred along the edges of eutectic cells due to the Zr enrichment.

The eutectic cells in IC-218 were destroyed by HT1, and they produced a distinct second phase, as

shown in Fig. 1b. Further heat treatment (HT2) did not change the microstructure produced by HT1 significantly. Pre-welding heat treatments changed not only the microstructure, but also Zr enrichment at dendrite boundaries. An analysis by EDX on dendrite boundaries and dendrite interiors in polished and etched specimens showed that while dendrite boundaries in all conditions were enriched with Zr, the specimens treated by HT2 had the highest Zr enrichment, and the as-cast ones had the lowest Zr enrichment, as shown in Table 1. As mentioned before, HT1 destroyed Zr-enriched eutectic cells in as-cast IC-218 and caused Zr to redistribute. Due to the limited solubility of Zr in the Ni_3Al alloy, Zr was prone to segregate at grain boundaries [17-19]. Therefore, HT1 increased Zr enrichment at dendrite boundaries. The higher Zr enrichment at dendrite boundaries resulting from HT2 was due to slight dendrite-boundary melting. Li et al. [20] showed that the dendrite-boundary melting temperature of IC-218 heat-treated using HT1 was about 1125°C.

3.2. Microstructure in the fusion zone

Weldability of IC-218 was found better than that of the single phase Ni_3Al alloy, IC-50, which is sensitive to macrocracking in the FZ and the HAZ [11-13]. No macrocrack was found in either the FZ or the HAZ. The FZ of IC-218 was characterized by a columnar-grain microstructure with second phase between the columnar grains, as shown in Fig. 2a. Micro-solidification cracks were occasionally found in the FZ along columnar grain boundaries (Fig. 2a). The microstructure in FZ was independent of pre-welding heat treatments because melting processes during welding eliminated the effect of the pre-welding microstructure on the post-welding microstructure in the FZ. Investigation by SEM at higher magnifications (3000X and higher) revealed that the second phase had striated eutectic structures, and some of the striated regions contained microcracks or a Zr-rich phase, as shown in Fig. 2b and 2c. Analysis by EDX showed the Zr-rich phase had an approximate composition of $Zr_{15}(Ni,Al,Cr)_{85}$,

indicating that it was a Ni-Ni_5Zr type eutectic that had a melting temperature of about 1175°C according to the equilibrium Ni-Zr phase diagram [21]. Analysis by EDX also showed 1.5 to 2.5 wt% Zr in the eutectic structure and very low Zr (not detectable by EDX) in the interior of the columnar grains. According to the solidification diagram of Ni-Al-Cr ternary alloys [16], IC-218 solidified first as a disordered γ phase, and the remaining liquid between dendritic arms then underwent a eutectic reaction of $L \rightleftarrows \gamma + \gamma'$. The remaining liquid with high Zr solidified last by Ni-Ni_5Zr eutectic reaction. Solidification cracks appear to be related to the Zr-rich phase because a Zr-rich phase usually was found in the crack path, as shown in Fig. 2d. This observation suggested that the solidification cracks were due to the low-melting Zr-rich phase between dendrites. The $(\gamma + \gamma')$ eutectic volume fraction in the FZ of IC-218 was about 30%. The better resistance to solidification cracking in the FZ of IC-218 than that of IC-50 could be attributed to the higher-volume fraction of the eutectic liquid because more liquid was available to share the welding stresses generated during welding cooling.

3.3. Liquation cracking in the HAZ of as-cast specimens

Li [15] showed that the microstructure of IC-218 could be changed by heat treatments, and that phase transformation started at about 1150°C during fast heating and cooling. Unlike IC-50, weldments of IC-218 exhibited a clear HAZ in which phase transformation took place, as shown in Fig. 3. From Fig. 3, one can see that some cracks in the HAZ developed along the original dendrite boundaries. The longest crack stretches about 1.3 mm from the fusion line (the border between the FZ and the HAZ). The columnar grains in the FZ developed in epitaxial growth, i. e., they grew as if they were an extension of the dendrites in the HAZ. The dendrite boundaries in the HAZ experienced incipient melting during the welding thermal cycle, and cracks developed along such dendrite boundaries, as shown in Fig. 4a. A Zr-rich phase identical to that in Fig. 2d was also found at some crack tips near the fusion line. At

a distance of about 1 mm from the fusion line, cracks occurred mainly at the edges of eutectic cells, as shown in Fig. 4b. Investigation by SEM revealed that some of the cracks did not separate completely, but were joined by small metal ligaments, as shown in Fig. 5. The above features indicated that microcracks in the HAZ were apparently associated with incipient melting of dendrite boundaries in the HAZ during welding, and the cracks formed at elevated temperature when dendrite boundaries were still in the liquid state. Such microcracks in HAZ were termed as "liquation cracks" and were caused by a liquid film forming at dendrite boundaries during welding and being unable to accommodate thermally-induced stresses during the post-welding cooling. Liquation cracking is common [22-24] during welding of Ni-base alloys. Various mechanisms have been proposed to explain the origin of liquid at grain boundaries. Accumulation of solute at grain boundaries during their migration can cause melting. During rapid heating, second-phase particles can melt (known as "constitutional liquation") [25] and wet the grain boundary when it sweeps the particles during its migration. Another mechanism is that, through pipe diffusion, solute atoms can be transferred from the FZ to the HAZ along the grain boundaries that are continuous across the fusion line.

Analysis by EDX on melted dendrite boundaries, liquation crack tips, and unbroken ligaments in microcracks showed Zr enrichment (about 2 to 3 wt%), suggesting that the sensitivity of IC-218 to liquation cracking was associated with Zr enrichment at dendrite boundaries. According to the Ni-Zr binary phase diagram [21], adding Zr decreases the melting temperature of a Ni-Zr alloy dramatically. By rapidly heating and quenching IC-218 from different temperatures, it was found that dendrite boundaries in as-cast IC-218 melted at about 1150°C [20], which is lower than that of the Ni-Zr eutectic temperature (1175°C). The reason leading to such a low temperature is not clear yet. B might contribute because B was found to increase the sensitivity of Ni-base superalloys to liquation cracking in the HAZ [26], and B in Ni_3Al alloys segregated at grain boundaries. The effect of B on grain

boundary melting in Ni_3Al alloys needs to be studied. Due to the higher Zr concentration at the edges of the eutectic cells in as-cast IC-218, the cells were prone to incipient melting, and consequently to liquation cracking.

3.4. Effect of pre-welding heat treatment on liquation cracking in the HAZ

Liquation cracks were also found in the HAZs of the specimens treated by HT1 and HT2. Liquation cracks developed along original dendrite boundaries, as shown in Fig. 6. Analysis by EDX on melted dendrite boundaries, crack tips, and unbroken ligaments in cracks also showed Zr enrichment. The frequency of liquation crack occurrence (FLCO) in HAZ was increased by HT1 and HT2. The FLCO was defined as the number of locations within 5 cm weld in which liquation cracks were found. Specimens treated by HT2 showed the highest FLCO (17±3/5 cm), and as-cast specimens had the lowest FLCO (12±3/5 cm), as shown in Table 2. From Table 2, it can be seen that crack numbers were related to the initial Zr enrichment at dendrite boundaries. The higher the Zr enrichment, the higher the FLCO.

4. Conclusions

1. As cast IC-218, a two phase Ni_3Al alloy, was characterized with coarse dendrites and many eutectic cells. Enrichment of Zr was found at the dendrite boundaries and the edge of eutectic cells.

2. Heat treatment of 1100°C/23 h/furnace-cool destroyed the eutectic cells and increased slightly the Zr enrichment at dendrite boundaries. An additional heat treatment of 1120°C/30 min/air-cool did not change the microstructure significantly, but did further increase the Zr enrichment at dendrite boundaries.

3. The fusion zone of the as-cast IC-218 alloy consisted of a columnar grain structure. A striated eutectic structure developed along the columnar grain boundaries. Some microcracks (2 to 5 μm long) and Zr-rich phases were found in the striated structure. Solidification cracks were occasionally found

along the columnar grain boundaries. A Zr-rich phase was usually found in the path along which a solidification crack developed. Pre-welding heat treatments had no effect on the microstructural characteristics in the fusion zone of the IC-218 alloy.

4. As cast IC-218 was highly susceptible to liquation cracks in the heat-affected zone. Liquation cracks developed along the original dendrite boundaries; some short liquation cracks also developed at the edge of eutectic cells in the base metal. Zr enrichment was observed in the liquated dendrite boundaries, crack tips and residual metal in liquation cracks in the heat-affected zone of as-cast IC-218.

5. While pre-welding heat treatments did not change microstructural characteristics in the fusion zone, the liquation crack density was increased in heat-affected zone. The increase in the crack density was due to the increase of Zr enrichment at dendrite boundaries due to the heat treatments.

Acknowledgement

We are grateful to Mr. P. Erfort of Armco Inc., Ohio, for providing the Ni_3Al alloy. The research was supported by the Division of Materials Science, Office of Basic Energy Science, U. S. Department of Energy under the Contract DE-AC06-76RLO-1830 with Battelle Memorial Institute.

References

1. S. M. Copley and B. H. Kear, *Trans. The Metall. Soc.-AIME, 239* (1967) 977.

2. C. T. Liu, in N. S. Stoloff, C. C. Koch, C. T. Liu and O. Izumi (eds.), *High Temperature Ordered Intermetallic Alloys II*, Materials Research Society, Pittsburgh, 1987, p. 355.

3. K. Aoki and O. Izumi, *Nippon Kinzoku Gakkaishi, 43* (1979) 1190.

4. C. T. Liu, C. L. White and J. A. Horton, *Acta Metall., 33* (1985) 213.

5. C. T. Liu, V. K. Sikka, J. A. Horton and E. H. Lee, in *Report No. 6483*, Oak Ridge National Laboratory, Oak Ridge, TN, August 1988.

6. C. T. Liu and V. K. Sikka, *J. of Metals, 38* (1986) 19.

7. V. K. Sikka, in S. H. Whang, C. T. Liu, D. P. Pope and J. O. Stiegler (eds.), *High Temperature Aluminides and Intermetallics*, Minerals, Metals and Materials Society, 1990, p. 505.

8. S. A. David, W. A. Jemian, C. T. Liu and J. A. Horton, *Welding Journal, 64* (1985) 22-s.

9. M. L. Santella and S. A. David, *Welding Journal, 65* (1986) 124-s.

10. M. L. Santella, J. A. Horton and S. A. David, *Welding Journal, 67* (1988) p. 63-s.

11. Huaxin Li and T. K. Chaki, in L. A. Johnson, D. P. Pope and J.O. Stiegler (eds.), *High Temperature Ordered Intermetallic Alloys IV*, Materials Research Society, Pittsburgh, 1991, p. 919.

12. Huaxin Li and T.K. Chaki, *Mater. Sci. Eng., A144* (1994), in press.

13. Huaxin Li and T.K. Chaki, in V. A. Ravi and T. S. Srivatsan (eds.), *Processing and Fabrication of Advanced Materials for High Temperature Applicatons--II*, TMS, 1993, p. 563.

14. Huaxin Li and T.K. Chaki, in I. Baker, R. Darolia, J. D. Whittenberger and M. H. Yoo (eds.), *High-Temperature Ordered Intermetallic Alloys V*, Materials Research Society, Pittsburgh, 1993, p. 1167.

15. Huaxin Li, Chapter 3, in *Ph. D. Thesis*, State University of New York at Buffalo, 1992.

16. A. Taylor and R. W. Floyd, *J. of the Inst. of Metals, 81* (1952) p. 451.

17. M. Morinaga, N. Yukawa and H. Adachi, *J. of the Physical Soc. of Japan, 53* (1984) 653.

18. T. H. Chuang, *Mater. Sci. Eng., A141* (1991) 169.

19. T. H. Chuang, Y. C. Pan and S. E. Hsu, *Met. Trans. A, 22A* (1991) 1801.

20. Huaxin Li and T.K. Chaki, *Mater. Sci. Eng.*, submitted for publication.

21. Ni-Zr Binary Phase Diagram, T. B. Massalski (ed.-in-chief), in *Binary Alloy Phase Diagrams*, 2nd ed., Vol. 3, Materials Park, Ohio, ASM International, December, 1990, p. 2890.

22. W. A. Owczarski, D. S. Duvall and C. P. Sullivan, *Welding Journal, 46* (1967) 423-s.

23. S. C. Ernst, W. A. Baeslack III and J. C. Lippold, *Welding Journal, 68* (1989) 418-s.

24. B. Radhakrishnan and R. G. Thompson, *Scripta Metall. Mat., 24* (1990) 537.

25. J. J. Pepe and W. F. Savage, *Welding Journal, 46* (1967) 411-s.

26. Manabu Tamuba, in John K. Tien and Thomas Caulfieled (eds.), *Superalloys, Supercomposites and Superceramics*, Academic Press, Inc., New Yowk, 1989, p. 215.

Table 1. Pre-welding heat treatments and Zr enrichment at dendrite boundaries

	As-Cast	HT1	HT2
DI*	1.169±.51	1.174±.12	.956±.03
DB**	1.323±.12	1.415±.11	1.488±.18
Zr_{DB}/Zr_{DI}	1.13	1.21	1.56
$(Zr_{DB}-Zr_{DI})/Zr_{DI}$	13.3%	20.5%	55.6%

* Dendrite interior; ** Dendrite boundary.

Table 2. Zr enrichment at dendrite boundaries and liquation cracks

	As-Cast	HT1	HT2
Zr_{DB}/Zr_{DI}*	1.13	1.21	1.56
$(Zr_{DB}-Zr_{DI})/Zr_{DI}$	13.3%	20.5%	55.6%
Crack #/5 cm**	12 ± 3	14 ± 2	17 ± 3

* DI and DB stand for dendrite interior and dendrite boundary, respectively.

** Crack number per 5-cm-long weldment.

Figure caption:

Fig. 1. Optical micrographs of IC-218. (a) As-cast specimen characterized with dendritic structure and eutectic cells. The arrow indicates the Zr-rich particles. (b) Specimen annealed at 1100^{o} for 23 h and furnace cooled. The eutectic cells disappeared.

Fig. 2. Microstructure of polished and etched surface of the FZ in as-cast IC-218. (a) Optical micrograph at low magnification. There is a solidification crack along columnar grain boundary. (b) and (c) SEM micrographs at high magnifications showing micro-cracks and high Zr phase (arrow pointed) in the striated structure. (d) High Zr phase (arrow pointed) in the path along which a solidification crack was developing.

Fig. 3. Optical micrograph showing the general features of the HAZ in as-cast IC-218. Liquation cracks developed along the original dendrite boundaries in the HAZ.

Fig. 4. Optical micrographs showing liquation cracks of the HAZ in as-cast IC-218. (a) Crack near fusion zone. The crack developed along the melted dendrite boundary. (b) Cracks at 1 mm away from fusion zone. The cracks mainly developed at the edges of the eutectic cells.

Fig. 5. SEM micrograph at high magnification showing the details of a liquation crack at an edge of a eutectic cell. The crack did not separate completely, but was joined by small metal ligaments that were enriched with Zr.

Fig. 6. Optical micrograph showing general features of the HAZ in IC-218 heat treated by 1100^{o}C/23h/furnace cool and 1120^{o}C/30min/air cool. Liquation cracks developed along the original dendrite boundaries in the HAZ.

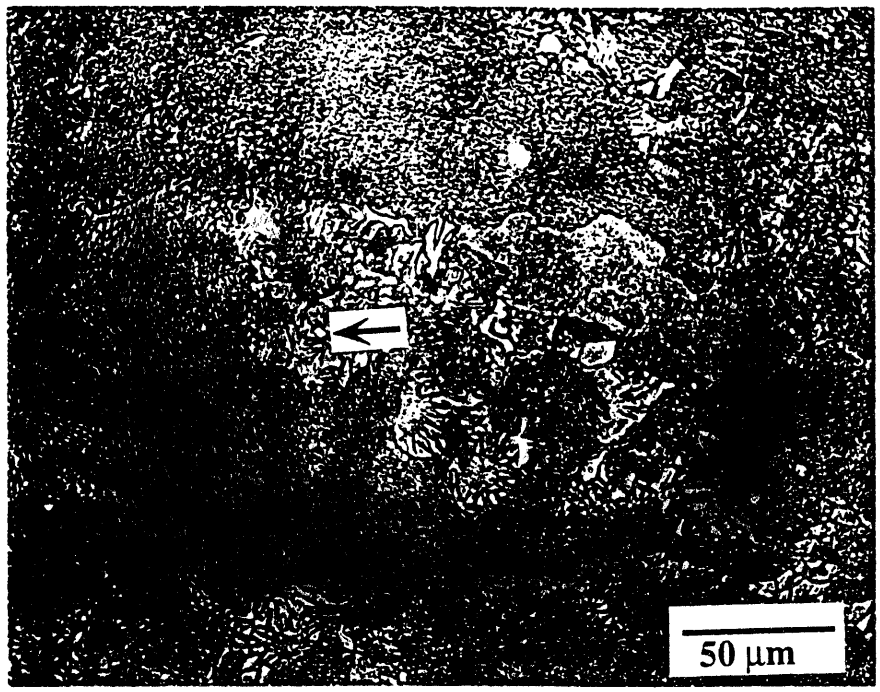

Fig. 1a

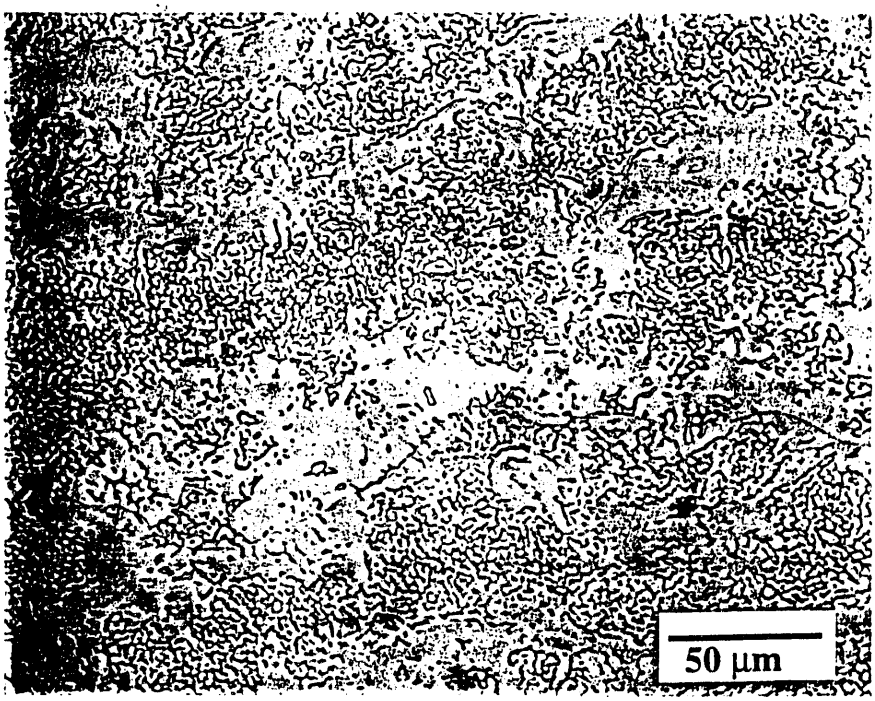

Fig. 1b

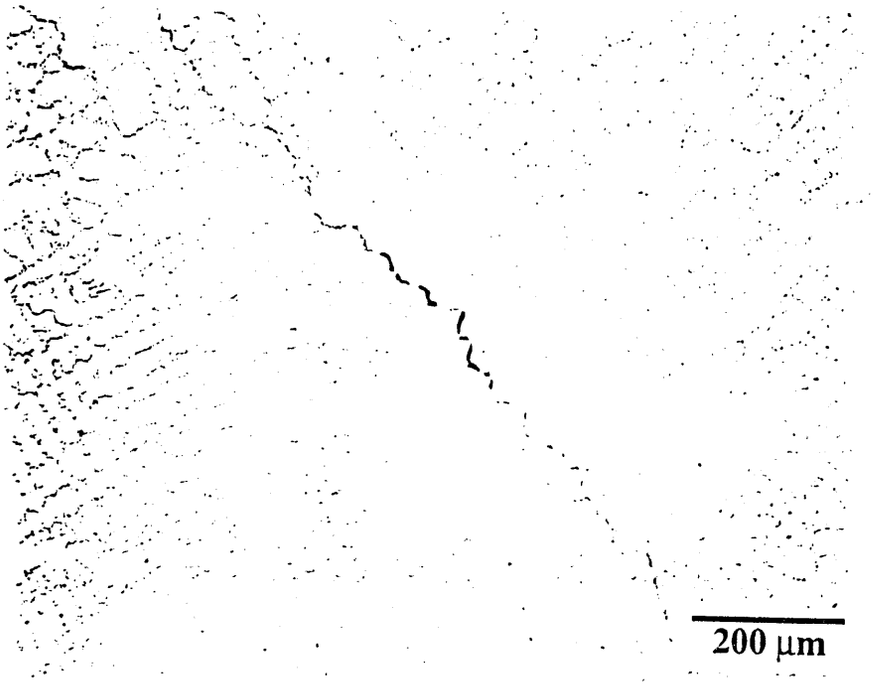

Fig. 2a

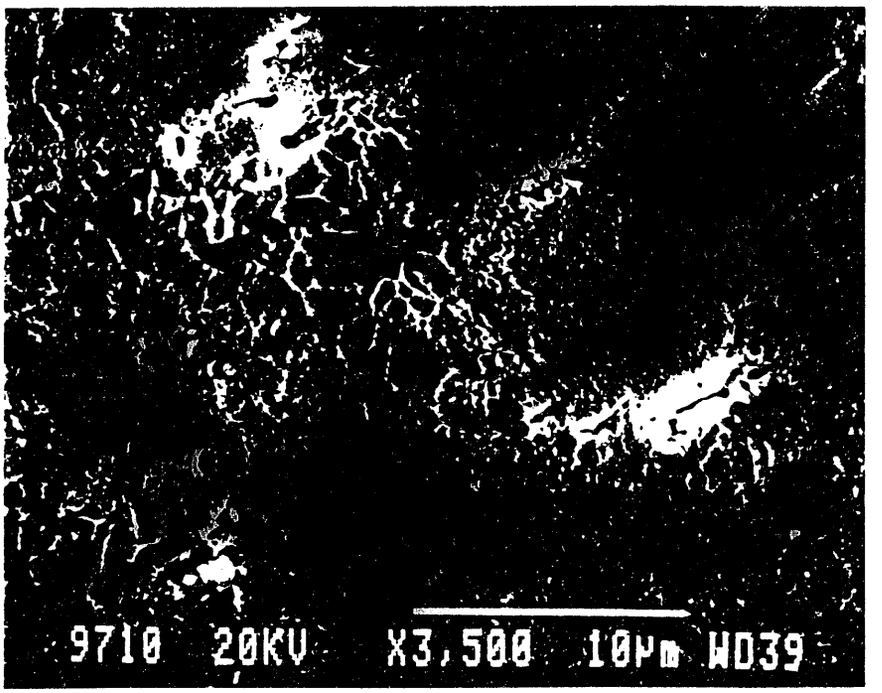

Fig. 2b

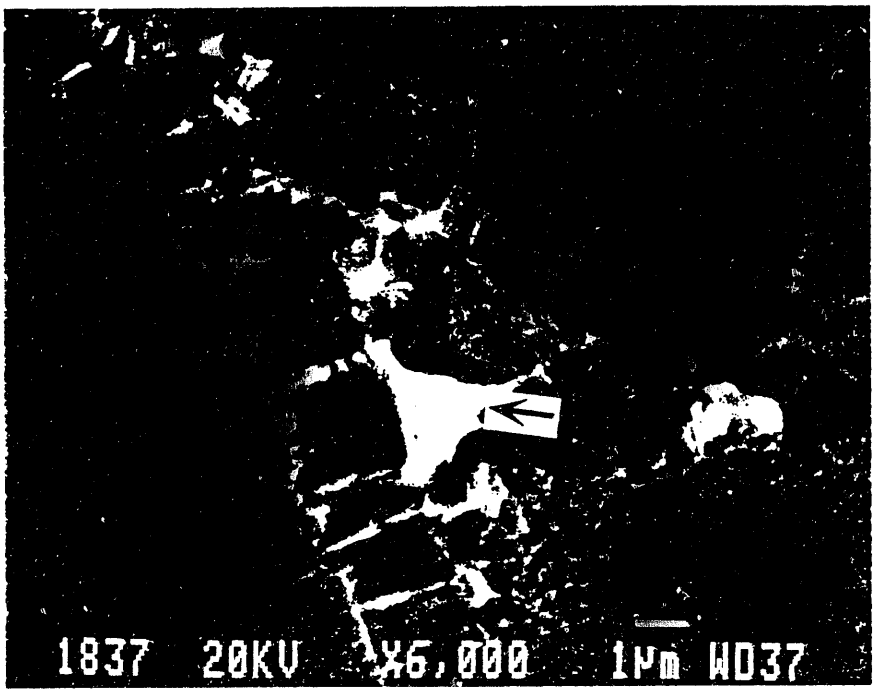

Fig. 2C

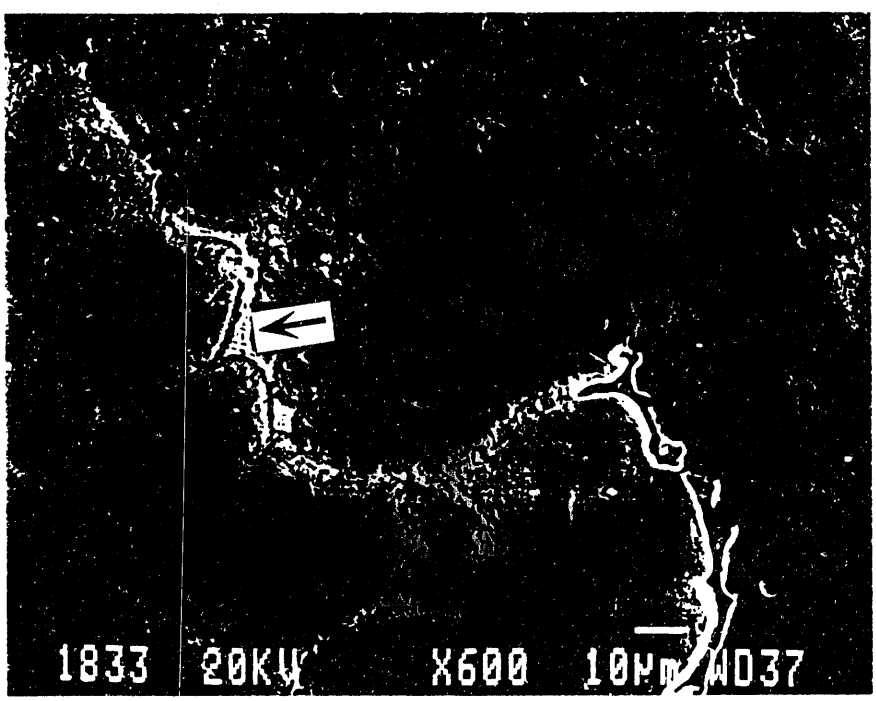

Fig. 2d

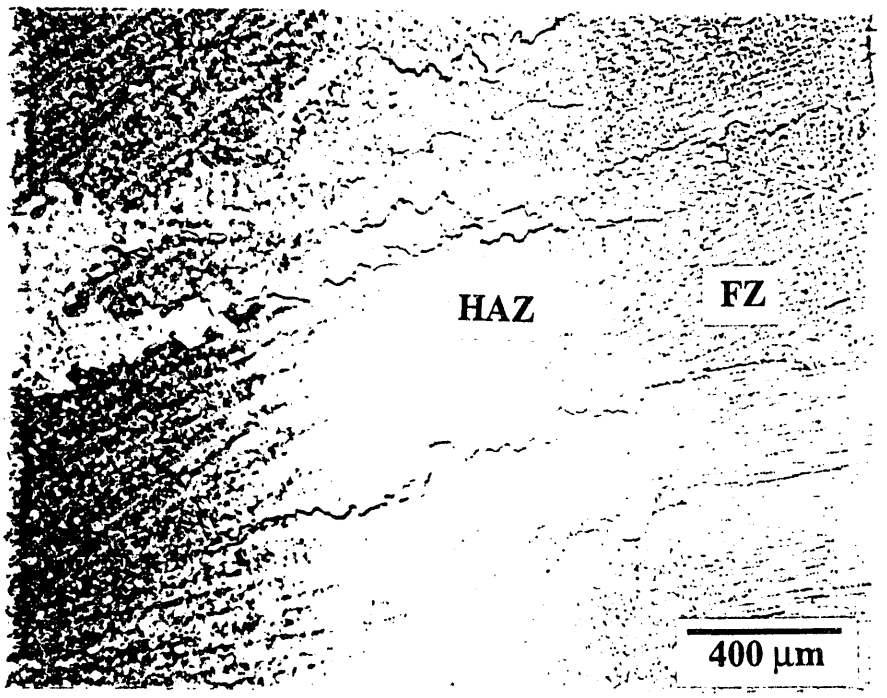

Fig. 3

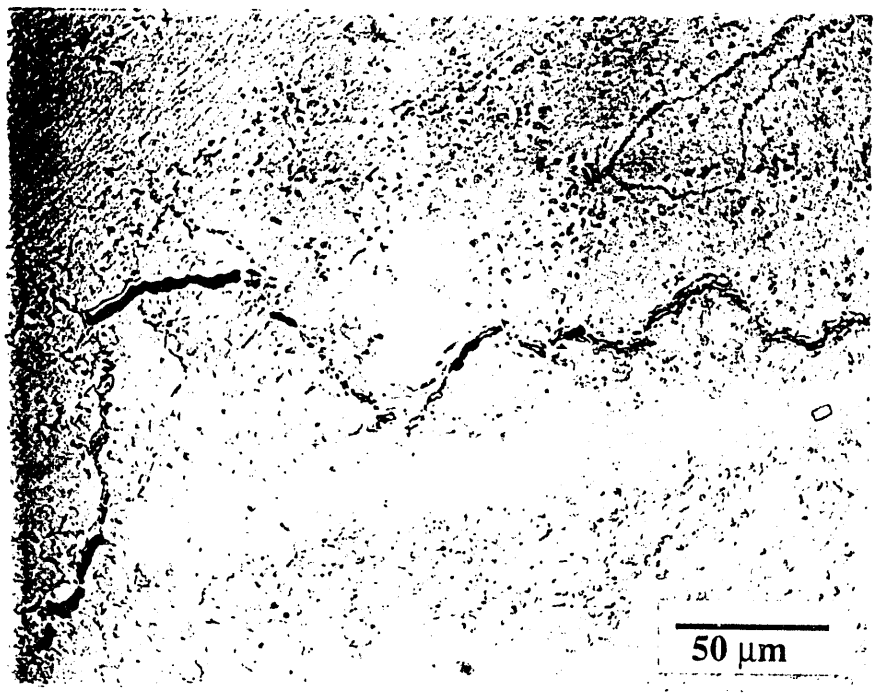

Fig. 4a

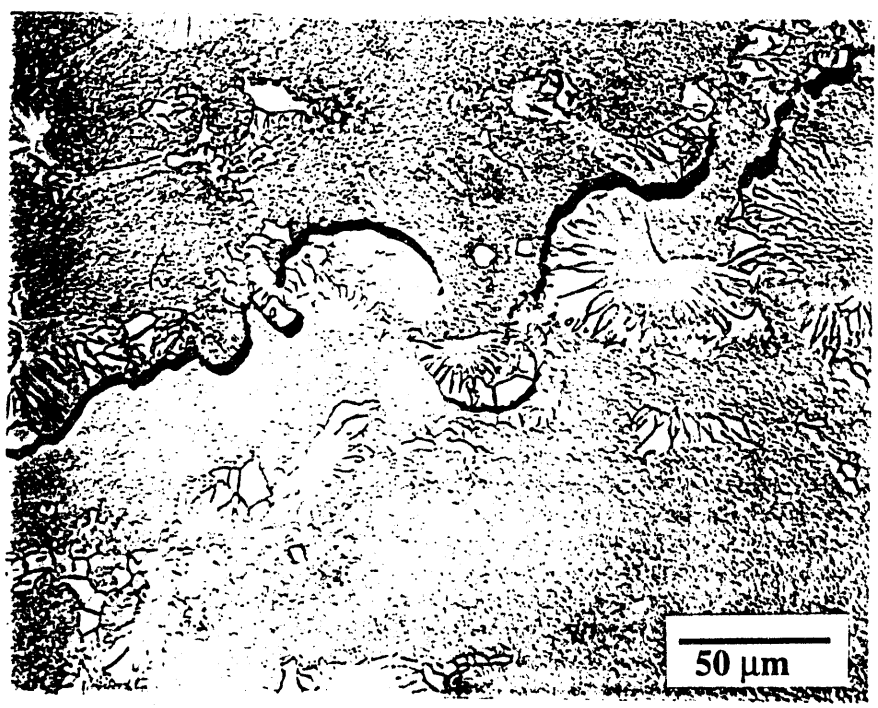

Fig. 4b

Fig. 5

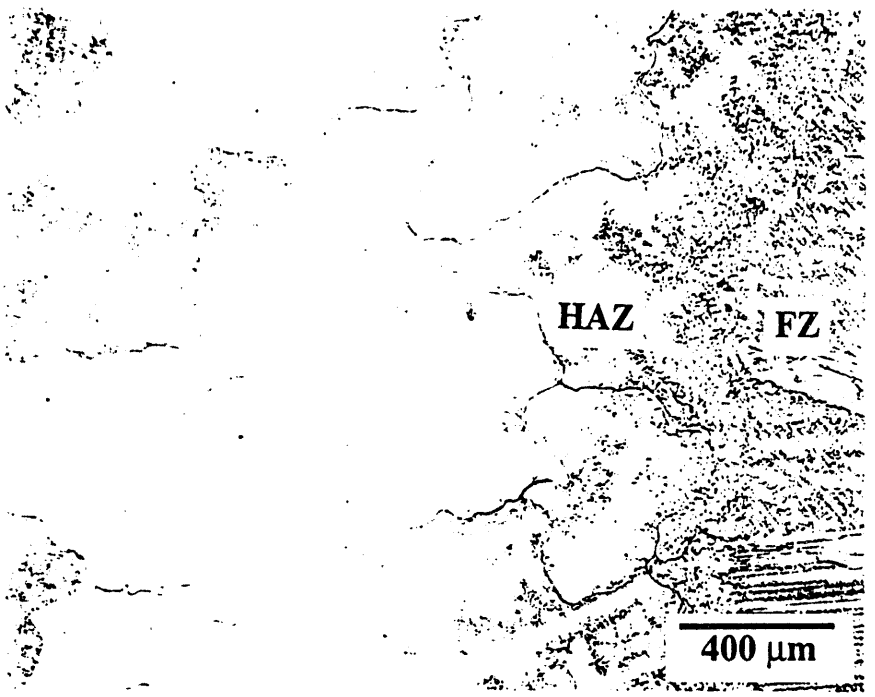

Fig. 6

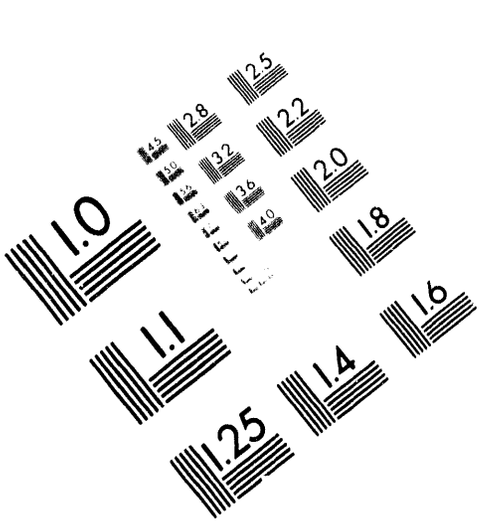

Association for Information and Image Management
1100 Wayne Avenue, Suite 1100
Silver Spring, Maryland 20910
301/587-8202

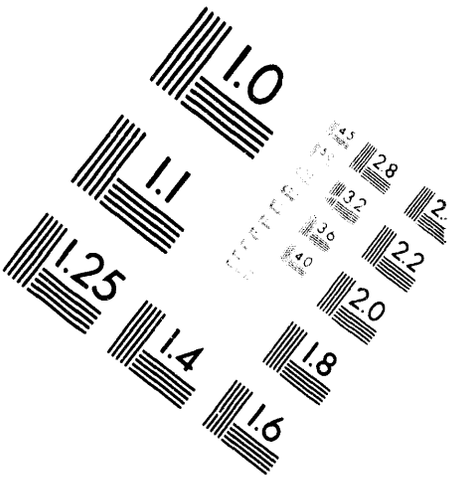

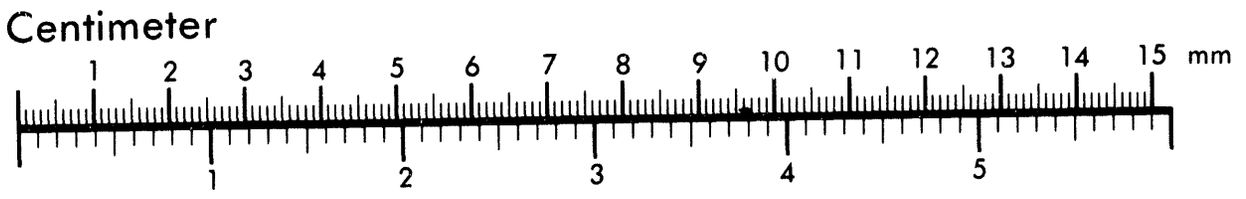

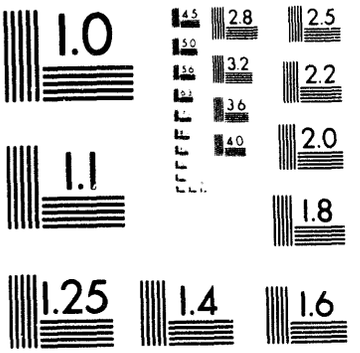

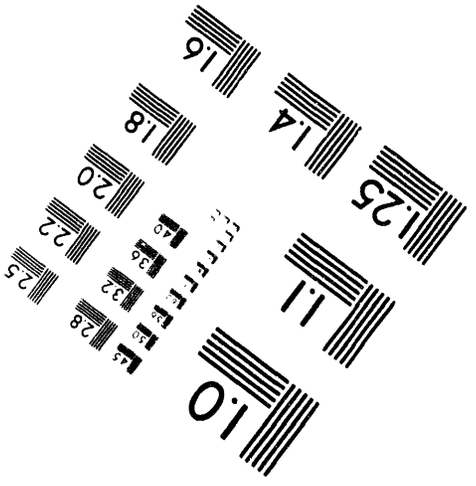

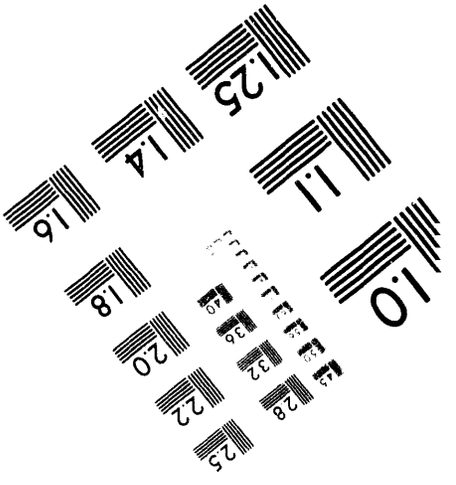

DATE FILMED

2/2/95

END